Cancer Management and Research

Dovepress

open access to scientific and medical research

Open Access Full Text Article

ORIGINAL RESEARCH

Downregulation of Immortalization-Upregulated Protein Suppresses the Progression of Breast Cancer Cell Lines by Regulating Epithelial–Mesenchymal Transition

This article was published in the following Dove Press journal:
Cancer Management and Research

Jialiang Wen*
Lizhi Lin*
Bangyi Lin
Erjie Xia
Jinmiao Qu
Ouchen Wang

Department of Thyroid and Breast Surgery, The First Affiliated Hospital of Wenzhou Medical University, Wenzhou, Zhejiang, People's Republic of China

*These authors contributed equally to this work

Introduction: Breast cancer (BC) is one of the most prevalent malignancies in women and its incidence has increased steadily over recent years (0.3% per year). However, the mechanism of BC tumorigenesis remains elaborate elucidation. With the aid of RNA sequencing technology, we discovered that immortalization-upregulated protein (*IMUP*) is overexpressed in BC tissues compared to normal breast tissues. Our study is to understand the role of *IMUP* in BC.

Methods: We validated the upregulation of *IMUP* from multiple public databases. By using quantitative real-time polymerase chain reaction (qRT-PCR), we proved that *IMUP* is overexpressed in BC tissues and cell lines. We performed proliferation, migration, invasion and apoptosis assays to explore the function of *IMUP* in BC cell lines (MCF-7 and MDA-MB -231). Besides, we investigated the effect of *IMUP* silencing on epithelial–mesenchymal transition using Western blotting and qRT-PCR.

Results and Discussion: We validated that *IMUP* expression in BC tissues and cell lines is higher than that in the normal control group. The clinical analysis showed that *IMUP* is associated with lymph node metastasis and the outcome of neoadjuvant taxol-based therapy. The loss of function assay demonstrated that, with silencing *IMUP*, the capacities of proliferation, migration, and invasion of BC cell lines were impaired, while the apoptosis rate of cells increased. Meanwhile, the downregulation of *IMUP* could hinder the procession of epithelial–mesenchymal transition.

Conclusion: Our study proved that *IMUP* plays a vital role in BC and acts as a potential target and marker in future therapy.

Keywords: immortalization-upregulated protein, IMUP, breast cancer, BC, progression, epithelial–mesenchymal transition, EMT

Introduction

Breast cancer (BC) is the biggest killer among women diagnosed with cancer worldwide. According to statistics by the American Cancer Society, in the United States, 276,480 estimated new cases of female BC that account for 30% of female cancer will be diagnosed and will cause over 40,000 deaths in 2020.[1] Based on hormone receptor (HR) and human epidermal growth factor receptor (HER2) status, BC is classified as HR+/HER2- (70%), ERBB2+ (15–20%) and triple-negative (HR-/HER2-, 15%) subtypes.[2] In recent years, many treatments for early BC determined by subclassification greatly improve the prognosis of BC patients with a 5-year survival

Correspondence: Ouchen Wang
Department of Thyroid and Breast Surgery, The First Affiliated Hospital of Wenzhou Medical University, Wenzhou 325000, Zhejiang, People's Republic of China
Tel +86 13957706099
Email woc@wmu.edu.cn

submit your manuscript | www.dovepress.com
DovePress
http://doi.org/10.2147/CMAR.S259526

rate of more than 85%.[3] For example, cyclin-dependent kinase 4/6 inhibitors and HER2-targeted agents have been proven to benefit early BC patients with high risk.[4,5] However, as for patients with advanced BC, the 5-year survival rate is less than 40%;[6] mainly due to the drug resistance, sustained tumor invasion, metastasis and evolution, all of which lead to tumor spread throughout the body, resulting in the death of patients.[7] Therefore, it is crucial for us to understand the occurrence and development of BC and to find a biomarker that indicates the sensitivity of current therapy and long-term outcome in the early stage of the disease.

To excavate new markers, we carried out RNA sequencing analysis of 20 pairs of BC tissues and adjacent normal tissues (unpublished data). We found that immortalization-upregulated protein (*IMUP*), a coding gene located on chromosome 19q13, also known as Hepatocyte Growth Factor Activator Inhibitor Type 2-Related Small Protein (*H2RSP*) or *C19orf33*, is upregulated significantly in BC tissues compared with noncancerous tissue. The two transcripts of *IMUP* were first identified in Simian virus 40-immortalized human fibroblasts by Seishi Kato.[8] The protein coded by *IMUP* plays a role in placental development and pre-eclampsia.[9,10] In the field of cancer research, *IMUP* was overexpressed in many gynecologic malignancies and associated with the prognosis of cervical squamous cell carcinoma.[11–13] Moreover, previous studies showed that *IMUP* expression was higher in multifocal BC than unifocal BC and might relate to an aggressive phenotype of BC cell lines.[14,15] However, the biological function of *IMUP* in BC still has not been systematically investigated yet.

In this study, we validated the upregulation of *IMUP* in BC tissues and cell lines. We also found that high expression of *IMUP* might correlate with lymph node metastasis (LNM) and worse response to taxol. Loss-of-function experiments revealed the biological function of *IMUP* in the BC cell line, as well as the relationship between *IMUP* and Epithelial–mesenchymal transition (EMT). All in all, our findings showed that *IMUP* could act as a tumor promoter, which implies that it might be a target for future treatment of BC.

Materials and Methods

Validated Samples

Forty-eight matched pairs of BC samples and adjacent normal tissue samples were collected from the Department of Thyroid and Breast Surgery of The First Affiliated Hospital of Wenzhou Medical University (Wenzhou, Zhejiang, China). Each Sample was initially snap-frozen in liquid nitrogen after excision of the tumor by the surgeon and stored at −80°C until use. The histological analysis of each specimen was verified by the pathologists who possess the title of director. Informed consent was obtained from all patients before tissue collection.

Public Datasets

The clinical information and the sequencing data of 1091 primary BC samples and 113 normal breast tissues were downloaded from The Cancer Genome Atlas (TCGA) breast cancer database (https://tcgadata.nci.nih.gov/tcga/). The information of isoforms from BC tissues was retrieved using GEPIA2 (http://gepia2.cancer-pku.cn/). Moreover, the mRNA expression of *IMUP* in other datasets was retrieved from the Oncomine online tool (https://www.oncomine.org). Microarray dataset GSE22513[16] downloaded from Gene Expression Omnibus (GEO) (https://www.ncbi.nlm.nih.gov/geo/) contained samples from BC patients who achieved a pathologic complete response (pCR) or non-pCR after treatment of neoadjuvant paclitaxel/radiation therapy. The differentially expressed genes (DEGs) filtered by the threshold of p-value < 0.05 and $|\log2(\text{fold change})| \geq 2$ were identified using Limma package by R software. The heatmap was performed using the Euclidean distance metric.

Cell Culture and Transfection

Human BC cell lines (MDA-MB-231, MCF-7, T47D, MDA-MB-436, MDA-MB-453) and normal mammary epithelial cell line (MCF-10A) were purchased from the Cell Bank of the Shanghai Chinese Academy of Sciences (Shanghai, China). Under 5% CO2, MDA-MB-231, MCF-7, and T47D were cultured in DMEM medium (Gibco, Invitrogen, Carlsbad, CA, USA), and the MCF-10A was cultured in DMEM-F12 medium (Gibco). MDA-MB-436 and MDA-MB-453 were incubated in L-15 medium (Gibco) without CO2. All cell lines were grown with 10% Fetal bovine serum (Gibco) and 1% penicillin/streptomycin (Solarbio, Beijing, China) at 37°C.

The cells (MCF-7 and MDA-MB-231) were seeded in 6-well plates before transfection at a certain density (15×10^4 cells per well). Small interfering RNA (siRNA) designed and supplied by Gene Pharma (Shanghai, China) was used to silence the expression of *IMUP*. After premixing with Lipofectamine RNAiMAX (Invitrogen, Grand Island, NY,

USA) (siRNA: iMAX= 10 ul/4 ul; 100 nM final concentration per well), the siRNA was introduced into cells. The medium was replaced after 7 h and further experiments could be conducted after 48 h. The siRNA sequences targeted *IMUP* were as follows: siRNA1- sense: GGUCCGGGUCC AAAGCAAGTT/antisense: CUUGCUUUGGACCCGGAC CTT; siRNA2- sense: GGAUGUGAAGUCCCACGCUTT/ antisense: AGCGUGGGACUUCACAUCCTT.

RNA Isolation and Quantitative Real-Time Polymerase Chain Reaction

The TRIzol reagent (Thermo Fisher Scientific, Waltham, MA, USA) was used to isolate the total RNA of tissues and cells according to the manufacturer's protocol. Reverse transcription was performed using ReverTra Ace qPCR RT Kit (Toyobo, Osaka, Japan) and its temperature protocol was as follows: 16°C for 5 min, 42°C for 30 min and 98°C for 5 min. The quantitative real-time polymerase chain reaction (qRT-PCR) was applied to measure mRNA expression using the SYBR Premix Ex Taq II kit (RR820A, TaKaRa, Dalian, China). The conditions of qRT-PCR in the ABI 7500 Real-Time PCR System (Thermo Fisher Scientific Inc) were: 95°C for 30 seconds, followed by 40 cycles of 95°C for 5 seconds and 60°C for 34 seconds. The $2^{-\Delta\Delta Ct}$ method was employed for data analysis. All experiments were repeated at least twice. The primers (Generay, Shanghai, China) involved in this study were as follows: *IMUP*- forward: GGTTTAAT GAGCCCTGTCC/reverse: CAAGAAGCCCAAAGTGAA GA; Isoform-1 (ENST00000301246) forward: GATGTGA AGTCCCACGCTGC/reverse: GCCTCCTTCTTCTTGCC CTT; Isoform-2 (ENST00000588605) forward: TCACTGC CGCACCTCCAT/reverse: CATCCGTGTCCGAATCGCT; *GAPDH*- forward: GTCTCCTCTGACTTCAACAGCG/ reverse: ACCACCCTGTTGCTGTAGCCAA; *E-cadherin*- forward: AGTCACTGACACCAACGATAAT/reverse: ATC GTTGTTCACTGGATTTGTG; *N-cadherin*- forward: CGA TAAGGATCAACCCCATACA/reverse: TTCAAAGTCGA TTGGTTTGACC; *Vimentin*- forward: CCGACACTCCTA CAAGATTTAGA/reverse: CAAAGATTTATTGAAGGAG AACC.

Cell Counting Kit-8 Assay and Colony Formation Assay

At 48 h after transfection, the cells were collected by digestion and centrifugation. MDA-MB-231 (2×10^3 cells per well) and MCF-7 (3×10^3 cells per well) were plated into 96-well plates. Cell Counting Kit-8 (CCK-8) (Beyotime Biotechnology, Shanghai, China) was used to assess cell viability every 24 h following protocol (10 ul per well). The cells were incubated at 37°C for 3 h and then the absorbance was read at 450 nm on a spectrophotometer. Additionally, Cells were also seeded in 6-well plates evenly with the number described above. At least 7 days later, colonies were fixed with 4% paraformaldehyde and stained by 0.1% crystal violet before photo and counting. The experiments were duplicated three times.

Transwell Migration and Invasion Assay

Cells were collected and placed on the upper chamber of Transwell (#3422, Corning, NY, USA) (4×10^4 cells per well for MDA-MB-231 and 1×10^5 cells per well for MCF-7) with the serum-free medium. The lower chamber contained 600 ul medium with 10% serum. The top surfaces of Transwell were wiped with cotton swabs and the lower sides were fixed by 4% paraformaldehyde and stained with 0.1% crystal violet after 24 h. Five random fields of each chamber were imaged under a microscope at ×20 magnification. Invasion assay was conducted using the Matrigel invasion chamber (#354,480, Corning Biocat, NY, USA) by the same protocol.

Wound Healing Assay

After transfection, cells were seeded in 24-well plates (2.5×10^5/well) with the serum-free medium and the pipette tip was used to create a scratch on each well. Five fixed points were imaged under a microscope at ×5 magnification at 0h and 24 h after scratching. ImageJ software (NIH, MD, USA) was used to quantify the migrating areas. The migrating rate (%)= (0 h wound area – 24 h wound area)/0 h wound area × 100%.

Apoptosis Assay

Annexin V FITC apoptosis kit (#556,547, BD, Franklin Lakes, NJ, USA) was used to detect cellular apoptosis by flow cytometry. The targeted cells were harvested and resuspended in 500 ul 1×bind buffer. Then the resuspended cells were stained with 5 ul Annexin V-FITC for 15 min and 5 ul PI for 5 min at room temperature. Flow cytometry (BD Biosciences AccuriC6, NJ, USA) adopted 2×10^4 labeled cells and determined the level of apoptosis. Flowjo software (FlowJo, Ashland, USA) was done to analyze the results. The apoptosis rate was identified as the proportion of late apoptotic cells (Q2, Annexin V+/PI +) and early apoptotic cells (Q3, Annexin V+/PI−).

Western Blotting

Cell protein was extracted using RIPA buffer (Solarbio, Beijing, China) with phenylmethanesulfonyl fluoride (Solarbio). Samples with 100 ul lysis buffer were incubated on ice for 30 min and then shook with ultrasound for 1 min. After centrifuging for 20 min, the protein concentration was measured by the bicinchoninic acid (BCA) assay (Thermo Scientific, USA). Samples with loading buffer were subjected to electrophoresis on 10% sodium dodecyl sulfate-polyacrylamide gel electrophoresis (BioRad, Berkeley, CA, USA), and transferred to polyvinylidene difluoride (PVDF) membranes (0.45 um, EMD Millipore, Billerica, MA, USA) at 300 mA for 2 h. The PVDF membranes were incubated at 4°C with primary antibodies overnight after blocking in 5% fat-free milk. The membranes were subsequently washed and blotted with corresponding horseradish peroxidase-conjugated secondary antibody (1:5000, Abcam, Cambridge, UK) at room temperature for 2 h. Next, the chemiluminescence (ECL) (Thermo Scientific, USA) detection system was performed to visualize the protein bands. The protein expression related to β-actin were quantified by ImageJ software. Every experiment was repeated independently at least two times. The primary antibodies used in this research were as follows: IMUP (1:1000, ab213949, Abcam, Cambridge, MA, USA), E-cadherin (1:5000, 20,874-1-AP, Proteintech, Wuhan, China), Vimentin (1:2000, 10,366-1-AP, Proteintech), N-cadherin (1:2000, 22,018-1-AP, Proteintech), β-Actin (1:5000, 60,008-1-Ig, Proteintech).

Statistical Analysis

Statistical evaluation was conducted using SPSS 22.0 software (IBM SPSS Inc, Chicago, USA) and Graphpad Prism8 software (GraphPad, CA, USA). For categorical variables, Pearson's chi-square test was applied. For numerical data, two groups with the normal distribution were analyzed by Student's *t*-test. Non-normal distributed data were compared using non-parametric statistic tests (Mann–Whitney test for unpaired data and Wilcoxon rank-sum test for paired data). Two-way ANOVA was used for multiple comparisons. The data were presented as mean ± standard deviation for continuous variables and frequency for categorical variables, and p-value < 0.05 was considered to be significant. The receiver operating characteristic (ROC) curve was plotted by Prism8 and the area under the ROC curves (AUC) was applied to assess the diagnostic value.

Result

IMUP is Overexpressed in BC

To verify the result of our RNA sequencing data of *IMUP* (Table S1), we download gene expression data of BC from The Cancer Genome Atlas. We found that the expression of *IMUP* was higher in 1091 primary BC tissues than 113 normal breast tissues in the TCGA database ($p< 0.0001$, Figure 1A). Moreover, we detected the mRNA level of *IMUP* by qRT-PCR in cell lines and validated tissues cohort. As shown in Figure 1B, *IMUP* was significantly upregulated in 48 tumor tissues compared to the matched paraneoplastic tissues ($p< 0.0001$). Next, we further retrieved the *IMUP* expression in the Oncomine database. Analysis of Curtis ($p< 0.0001$),[17] Ma ($p< 0.01$)[18] and Richardson ($p< 0.05$)[19] showed that the mRNA expression of *IMUP* was higher in invasive BC tissue compared with nontumor samples (Figure 1CE). In BC cell lines, The *IMUP* mRNA expression in MDA-MB-231 ($p< 0.001$), MCF-7 ($p< 0.01$) and T47D ($p< 0.01$) were higher than the normal breast cell line MCF-10A, while the expression in MDA-MB-436 ($p< 0.01$) and MDA-MB-453 ($p< 0.01$) were lower than MCF-10A (Figure 1F). Finally, we evaluate the diagnostic effect in large sample size data; ROC curve analysis showed a certain diagnostic value of *IMUP* expression for discriminating BC from normal tissues in the TCGA (AUC:0.692, $p< 0.0001$) and Curtis cohorts (AUC:0.698, $p< 0.0001$) (Figure 1G). Taken together, these results demonstrated the marked upregulation of *IMUP* in BC.

High Expression of IMUP is Associated with Lymph Node Metastasis and Might Be a Predictive Biomarker for Worse Response to Neoadjuvant Paclitaxel-Based Therapy in BC

To explore the relationship between expression of *IMUP* and clinical features of BC patients, the tumor samples from TCGA and validated cohort were divided into two groups with high and low *IMUP* expression according to the median value. For TCGA cohort, as shown in Table 1, high expression of *IMUP* correlated with gender ($p< 0.001$), age ($p= 0.012$), LNM ($p= 0.012$) and disease stage ($p= 0.046$). For the validated cohort, the same relationship between *IMUP* expression and LNM was observed ($p= 0.042$, Table 2). Then we discovered that the *IMUP* expression in patients with LNM was higher

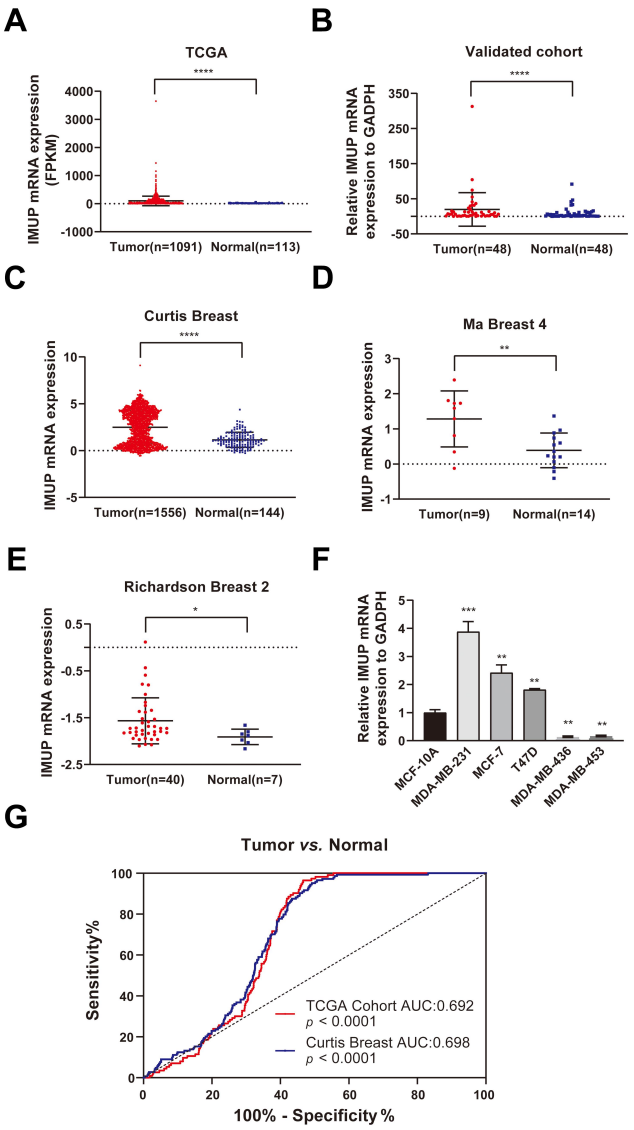

Figure 1 *IMUP* was upregulated in BC. (**A**) *IMUP* expression was higher in BC tissues compared to the adjacent normal tissues in the TCGA database. (**B**) The high expression of *IMUP* in BC was verified in the validated cohort by qRT-PCR. The mRNA expression of *IMUP* was upregulated in invasive BC compared with normal breast tissues in Curtis (**C**), Ma (**D**), and Richardson (**E**) BC databases. (**F**) The expression of *IMUP* in BC cell lines. Compared to the normal BC cell line MCF-10A, *IMUP* expression was higher in BC cell lines (MDA-MB-231, MCF-7, T47D) and lower in others (MDA-MB-436, MDA-MB-453). (**G**) ROC curve analysis showed that *IMUP* could distinguish patients with BC from nontumor patients in the TCGA and Curtis cohorts. Statistical analysis was illustrated as follows: (**A, C, E**): Mann–Whitney test; (**B**): Wilcoxon test; (**D** and **F**): *t*-test. *$p < 0.05$; **$p < 0.01$; ***$p < 0.001$, ****$p < 0.0001$.

than that in patients without LNM in TCGA and validated cohort (Figure 2A and B, $p< 0.05$).

To further investigate the clinical value of *IMUP*, we mined human BC samples from the GEO database. GSE22513, a dataset that aimed to identify molecular markers of pathologic response to neoadjuvant paclitaxel/radiation treatment, consists of 28 BC samples, which were obtained before treatment from 4 patients that achieved the pCR and 10 patients that achieved the non-pCR (2 replicates each). Heatmap of the top 50 DEGs ($p< 0.05$ and log2|[fold change]| ≥ 2) between the pCR group and the non-pCR group was shown in Figure 2D. The expression of *IMUP* was significantly higher in the non-PCR group compared to the pCR group (log2|[fold change]|= 2.534, $p< 0.001$, Figure 2C).

To sum up, the above discoveries indicated that *IMUP* might be a potential biomarker for the prediction of LNM and the effect of taxol.

The Expression of Isoforms of IMUP is Different in BC

The *IMUP* has two main isoforms produced by alternative splicing events. We evaluated the expression of isoform-1 (ENST00000301246.9) and isoform-2 (ENST00000588605.5) using the TCGA-based tool GEPIA2. We found that the isoform-1 level is higher than the isoform-2 level in BC tissues (Figure 3A). According to Figure 1F, MDA-MB-231 and MCF-7 who both expressed the highest levels of *IMUP* were selected for further experiments. Next, we explored the variant expression in BC cell lines and discovered that isoform-1 expression is significantly higher than isoform-2 expression in both MDA-MB-231 and MCF-7 ($p< 0.01$, Figure 3B). To further investigate the underlying biological function of *IMUP* in BC, We used two siRNA sequences to silence the expression of *IMUP*. The mRNA and protein levels of IMUP were markedly decreased in cells transfected with siRNA compared to that in the control group (Figure 3C and F). We also found that both isoform-1 and isoform-2 were significantly downregulated after transfection (Figure 3D and E).

Downregulation of IMUP Suppresses Tumor Proliferation and Induces Apoptosis in vitro

We performed CCK8 assay and colony formation assay to assess the effect of *IMUP* on cell proliferation. As shown in Figure 4A and B, knockdown of *IMUP* impaired the proliferative capacity of MDA-MB-231 and MCF-7. Evading apoptosis was proven to be a hallmark of cancer in the previous study.[20] Therefore, we further detected the level of apoptosis in BC cell lines. The results showed the increased apoptosis rate in IMUP-silence BC cells compared with control cells (Figure 4C). These findings indicated that *IMUP* could promote the proliferation and reduce apoptosis of breast cancer cell lines.

Table 1 The Correlation Between *IMUP* Expression and Clinicopathologic Features in the TCGA Cohort

Features	Patients	High Expression (%)	Low Expression (%)	Pearson X2	*p*
Gender					
Male	12	12(100.0)	0(0.0)	12.134	<0.001
Female	1078	533(49.4)	545(50.6)		
Age					
<50	299	131(43.8)	168(56.2)	6.309	0.012
≥50	791	414(52.3)	377(47.7)		
Tumor size (mm)					
≤20	279	140(50.2)	139(49.8)	0.008	0.930
>20	808	403(49.9)	405(50.1)		
Lymph node metastasis					
No	514	234(45.5)	280(54.4)	6.355	0.012
Yes	556	296(53.2)	260(46.8)		
Disease stage (AJCC7)					
I+II	805	386(48.0)	419(52.0)	3.990	0.046
III+IV	273	150(54.9)	123(45.1)		
Distant metastasis					
No	907	452(49.8)	455(50.2)	0.191	0.662
Yes	22	12(54.5)	10(45.5)		
Recurrence					
No	1016	506(49.8)	510(50.2)	0.232	0.630
Yes	74	39(52.7)	35(47.3)		

Note: P-value< 0.05.
Abbreviations: IMUP, immortalization-upregulated protein; TCGA, The Cancer Genome Atlas; Pearson X2, Pearson's chi-square; AJCC7, American Joint Committee on Cancer 7th edition.

Table 2 The Relationship Between *IMUP* Expression and Clinicopathologic Features in the Validated Cohort

Features	Patients	High Expression (%)	Low Expression (%)	Pearson X2	*p*
Age					
<50	22	11(50.0)	11(50.0)	0.000	1.000
≥50	26	13(50.0)	13(50.0)		
Tumor size (mm)					
≤20	28	12(49.9)	16(57.1)	1.371	0.242
>20	20	12(60.0)	8(40.0)		
Lymph node metastasis					
No	27	10(37.0)	17(63.0)	4.148	0.042
Yes	21	14(66.7)	7(33.3)		
Disease stage (AJCC7)					
I	21	8(38.1)	13(61.9)	2.116	0.146
II+III	27	16(59.3)	11(40.7)		
Degree of differentiation					
Low	17	6(35.3)	11(64.7)	3.741	0.053
Medium and high	26	17(65.4)	9(34.6)		
Ki67(%)					
<30	19	9(47.4)	10(52.6)	0.174	0.676
≥30	28	15(53.6)	13(46.4)		

Note: P-value< 0.05.
Abbreviations: IMUP, immortalization-upregulated protein; Pearson X2, Pearson's chi-square; AJCC7, American Joint Committee on Cancer 7th edition.

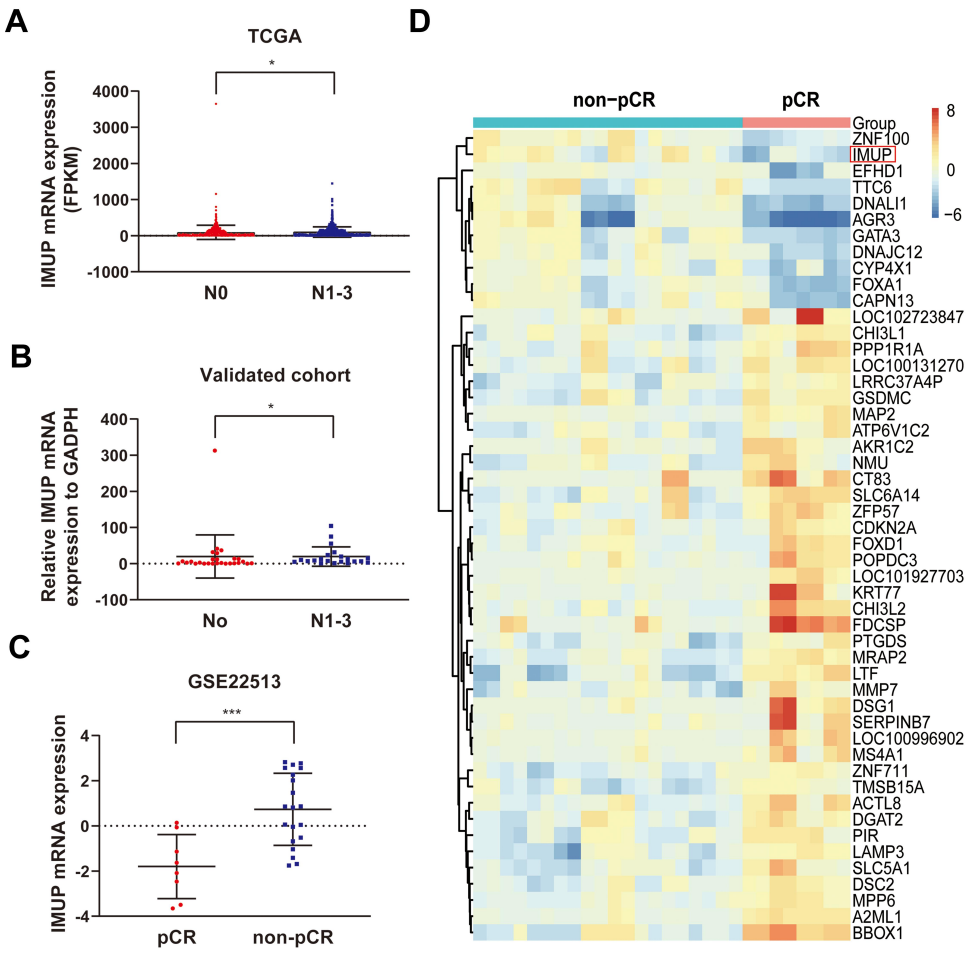

Figure 2 The expression of *IMUP* was associated with LNM and response to neoadjuvant taxol-based therapy. (**A**) The expression levels of *IMUP* were higher in the group with LNM compared to that in the group without LNM in the TCGA cohort. (**B**) The expression levels of *IMUP* were higher in the group with LNM compared to that in the group without LNM in validated cohort. (**C**) The expression of *IMUP* was elevated in the non-pCR group compared to the pCR group. (**D**) Heatmap of the top 50 significantly differential genes between the pCR group and the non-pCR group were identified from GSE22513. Statistical significance of differential expression was evaluated using Mann–Whitney test (**A** and **B**) and *t*-test (**C**) with p-value significant codes: *$p < 0.05$; ***$p < 0.001$.

The Downregulation of IMUP Hinders Migration and Invasion of BC Cell Lines

We had demonstrated that the expression of *IMUP* correlated closely to the LNM of BC. Thus, migration and invasion assay was conducted in MDA-MB-231 and MCF-7 to examine the effects of *IMUP* on cell motility. As shown in Figure 5A and B, wound healing assay and Transwell assay showed that migratory abilities in cells with a low level of *IMUP* decreased. The invasive properties of BC cell lines reduced by the downregulation of *IMUP* were analyzed by the Matrigel invasion chamber assays (Figure 5C). Combined with our conclusion above, *IMUP* might promote LNM by regulating BC cell migration and invasion.

IMUP Regulates the EMT Process of BC Cell Lines

Our work suggested that *IMUP* promotes an invasive phenotype in BC cells. Since the EMT process serves a critical role in tumor metastasis,[21] we hypothesized that *IMUP* might be involved in EMT during cell migration. Next, EMT-related gene expression (E-cadherin, N-cadherin, and Vimentin) were examined by qRT-PCR and Western blotting. The results showed that downregulated *IMUP* increased E-cadherin expression while decreasing the level of N-cadherin and Vimentin (Figure 6A and B). This evidence indicated that *IMUP* might regulate the progression of BC cell lines by EMT.

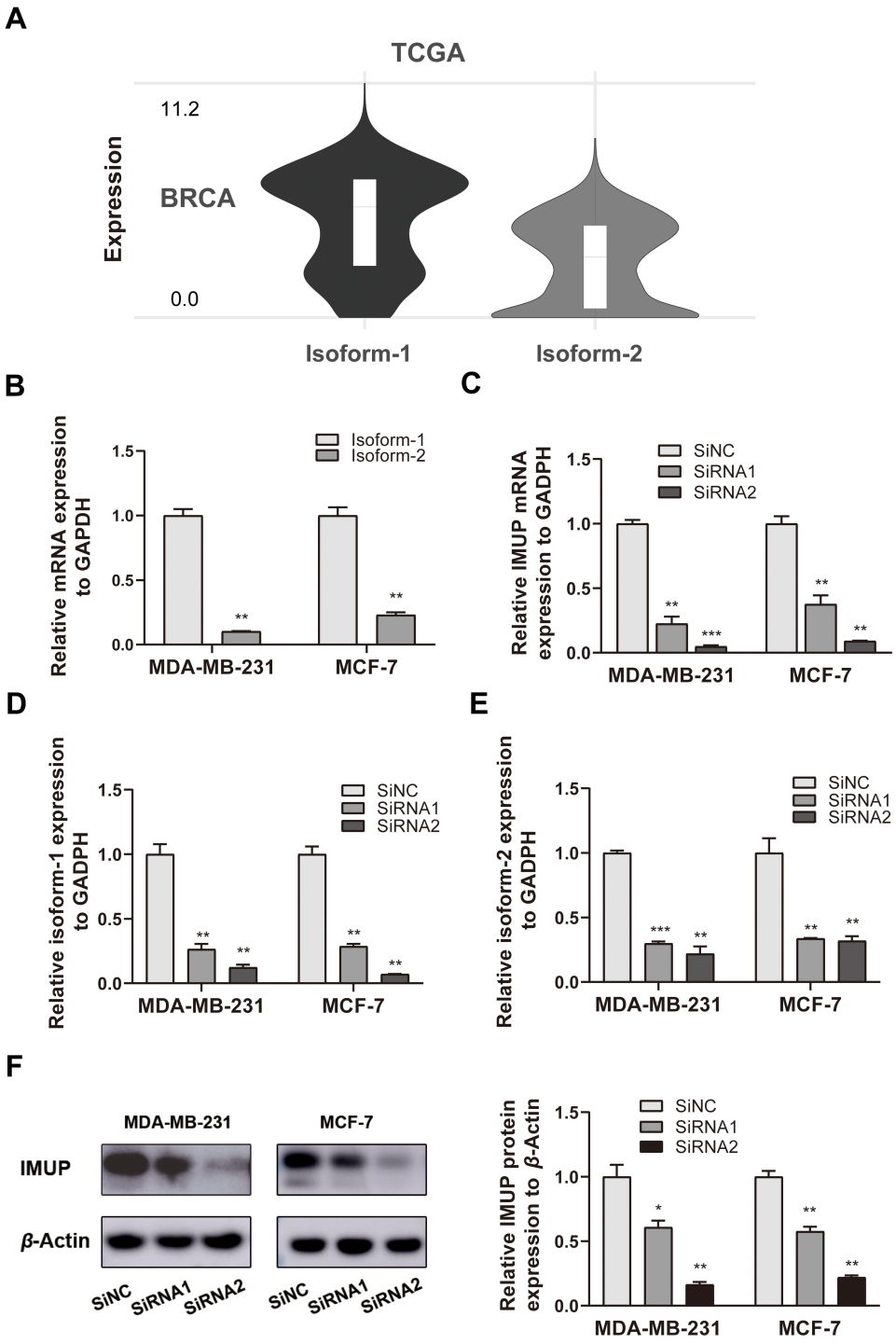

Figure 3 The isoform expression of *IMUP* in BC. (**A**) The isoform-1 expression was higher than isoform-2 expression in BC tissues from the TCGA database. (**B**) The isoform-1 expression was higher than isoform-2 expression in BC cell lines (MDA-MB-231 and MCF-7). (**C**) Compared to the level in the negative control (siNC) group, the mRNA expression of *IMUP* in siRNA1 and siRNA2 group was significantly lower in MDA-MB-231 and MCF-7. (**D** and **E**) The two isoforms are both downregulated significantly in cells transfected with siRNA. (**F**) The protein levels of IMUP in siRNA1 and siRNA2 group was significantly lower in MDA-MB-231 and MCF-7 compared to that in control. The Student's *t*-test was used for analyses. BRCA: breast invasive carcinoma. p-value significant codes: **p* < 0.05; ***p* < 0.01; ****p* < 0.001.

Discussion

Tremendous heterogeneity that results from the occurrence of clonal evolution and various genetic alterations complicates the treatment in BC.[22] Therefore, exploring new molecular markers that predict prognosis of the disease and understanding the underlying mechanisms of BC

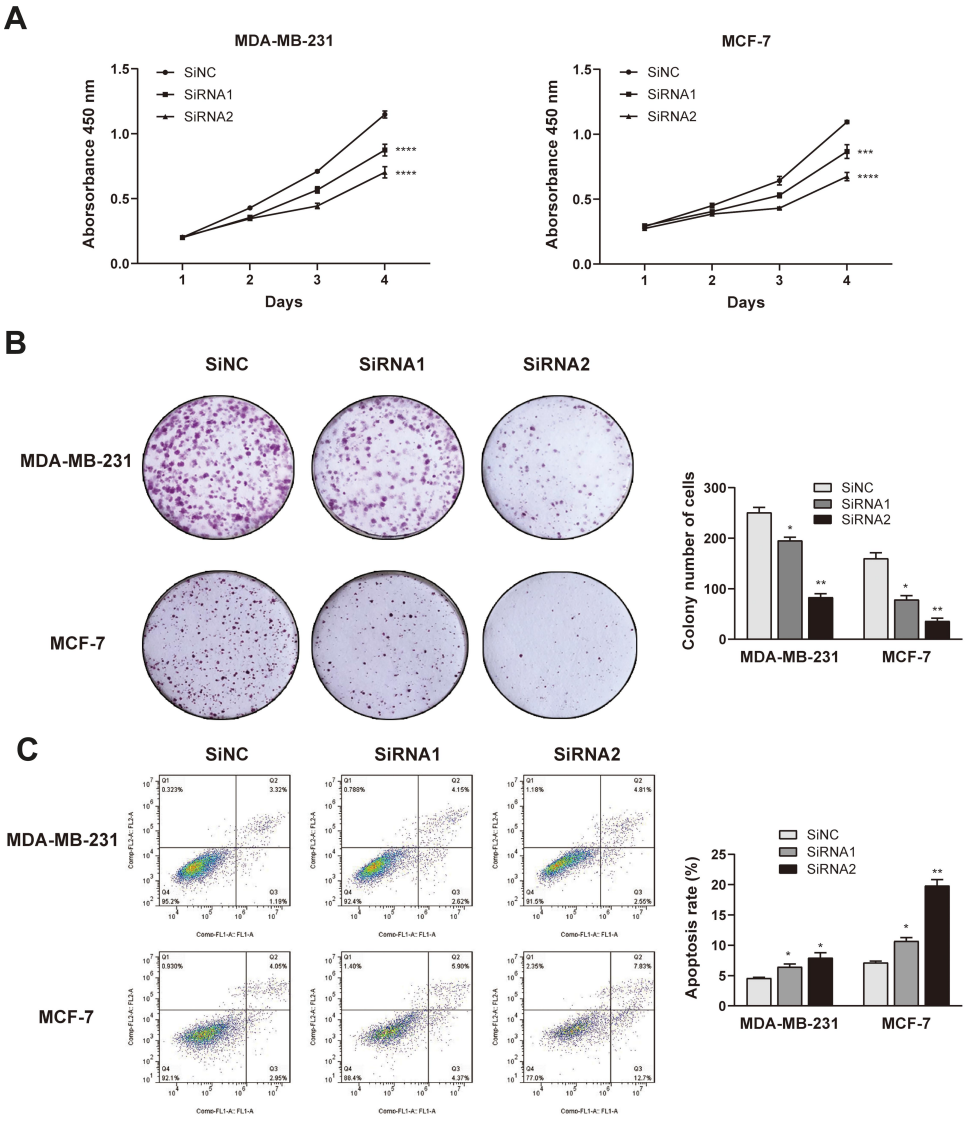

Figure 4 *IMUP* promoted proliferation and inhibited apoptosis in vitro. (**A** and **B**) CCK-8 assays and colony formation assays in MDA-MB-231 and MCF-7. Cells transfected with siRNA targeting *IMUP* suppressed cell proliferation. (**C**) Silencing *IMUP* promoted the apoptosis of BC cell lines. The Annexin V-FITC staining (FL1 channel) was taken as the horizontal coordinates and the PI staining (FL2 channel) was plotted on the ordinate. The apoptosis rate was the sum of the early apoptotic cells (Q3) and late apoptotic cells (Q2). Two-way ANOVA was applied to analyze the CCK-8 assay and the Student's *t*-test was used for others with p-value significant codes: *$p < 0.05$; **$p < 0.01$; ***$p < 0.001$, ****$p < 0.0001$.

could help us approach the individualized and precision treatment. According to our RNA sequencing data, we identified that *IMUP* was one of the most significant differentially expressed genes in BC. The expression of *IMUP* was shown to be upregulated in various cancers.[11,12,23] Existing studies have suggested that *IMUP* is associated with aggressive and malignant characteristics of BC.[14,15] However, little is known about the specific function of *IMUP* in BC. Here, we identified the upregulation of *IMUP* in BC in a public database, then reconfirmed the expression of *IMUP* in our validated cohort and BC cell lines using qRT-PCR.

Next, we investigated the relationship between *IMUP* expression and clinicopathological characteristics. The results revealed that the expression of *IMUP* relates to LNM and the response to neoadjuvant taxol therapy. Taxol is an effective agent in the first-line adjuvant or neoadjuvant chemotherapy for BC.[24,25] In recent years, the wild-spread application of neoadjuvant therapy (NAT) has increased the rate of breast-conserving surgery and offered chances in testing drug sensitivity. NAT has become a preferred treatment, especially for locally advanced BC.[26] Not only that, but numerous studies have also demonstrated that patients who achieve pCR

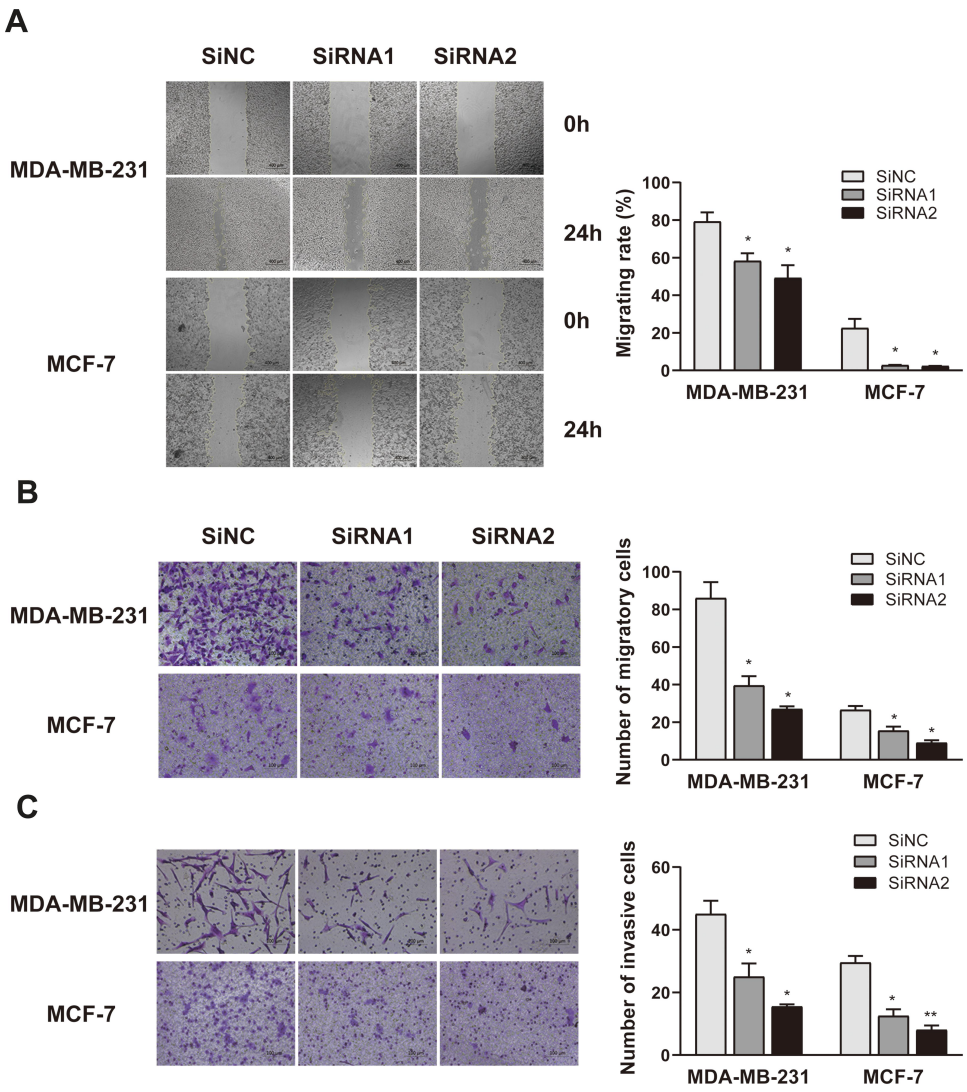

Figure 5 Down-regulation expression of *IMUP* hindered migration and invasion of BC cell lines. (**A**) Wound-healing assay determined the migratory ability of BC cell lines transfected with siRNA or siNC. The migrating rate (%)= (0 h wound area – 24 h wound area)/0 h wound area × 100%. (**B** and **C**) Transwell migration and invasion assays in the IMUP-silence group and their corresponding siNC group. The columns represented the mean of migrating or invasive cell numbers from experiments repeated at least twice. *$p < 0.05$; **$p < 0.01$, in comparison with the siNC group using Student's *t*-test.

following NAT had better overall survival.[27] Several genomic and proteomic signatures, such as PI3K mutations and MYC amplification, had been considered as valuable prognostic predictors in NAT.[28,29] Through data mining, we found that IMUP is a higher expressed gene in non-pCR versus pCR tumors following neoadjuvant taxol-based therapy, which suggested that its expression may affect taxol sensitivity in BC tumors and may serve as a predictor of response to NAT. Future research could continue to explore how the *IMUP* influences the tumor sensitivity to taxol and to validate its predictive value in other clinical cohorts.

Alternative RNA splicing is a common phenomenon in the post-transcriptional process. The variants form the same precursor can have different effects on cancers.[30] There are two main isoforms of *IMUP*. In our study, we found that isoform-1 (ENST00000301246) expressed highly in BC tissues and cell lines, and might play the leading role in the influence of *IMUP* on BC. The loss-of-function study showed that *IMUP* could promote proliferation, migration, and invasion while hindering apoptosis in vitro. EMT is a crucial process involving in cancer metastasis, progression, drug resistance, angiogenesis, and stemness.[21] David Sarrio reported that the elevation of EMT mesenchymal markers (Vimentin, N-cadherin, and Cadherin-11) together with the down-regulation of epithelial markers (E-cadherin and cytokeratins) occur in BC.[31] Moreover, multiple studies have

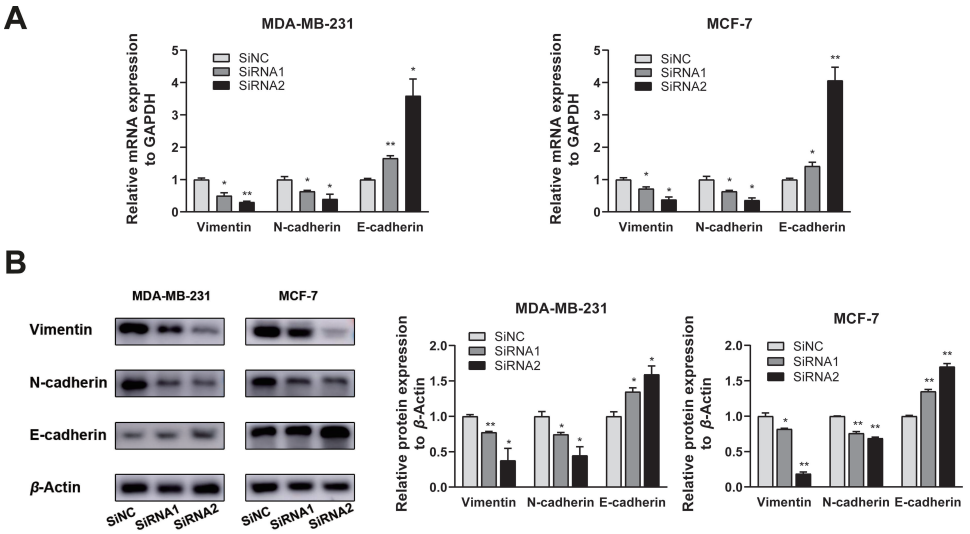

Figure 6 The downregulation of *IMUP* prevented EMT of BC cell lines. (**A**) The qRT-PCR analysis showed that silenced *IMUP* regulated the mRNA level of EMT-related molecules. Downregulation of *IMUP* elevated the expression of *E-cadherin* and decreased the expression of *N-cadherin* and *Vimentin*. (**B**) Western blotting assays showed that dysregulation of *IMUP* regulated EMT-related protein. Silencing *IMUP* led to the upregulation of the E-cadherin and downregulation of N-cadherin and Vimentin. Comparisons of grey value were performed using Student's *t*-test. *$p < 0.05$; **$p < 0.01$.

proved that EMT induction was an indicator of the enhancement of taxol resistance in BC.[32,33] Given the association of *IMUP* with cell motility and treatment response of taxol, we detected the levels of EMT-related genes in mRNA and protein levels. The results showed the lower Vimentin and N-cadherin expression and the higher E-cadherin expression in *IMUP*-knockdown BC cell lines compared to that in the control group. Our experiments suggested that *IMUP* might promote the progression of BC via regulating EMT procession.

Despite our novel findings, there are still some limitations to this research. First, the protein level of *IMUP* in BC tissues should be validated. Second, it is more convincing to assess the gain of function of *IMUP* in cell lines with low-level expression. In addition, biological examinations should be conducted to verify the *IMUP*-mediated effect on drug resistance. Finally, the results of the function of *IMUP* in BC need deeper validation in vivo.

Conclusions

In our present work, we conclude that *IMUP* is upregulated in BC and its expression is associated with LNM and the response to taxol therapy. *IMUP* silencing hinders the progression and reverses the EMT process in BC cell lines. These consequences indicate that *IMUP* functions as an oncogene and may be a potential therapeutic target in BC.

Data Sharing Statement

Raw data that supports the conclusions of this study are available on the main electronic data storage system of The First Affiliated Hospital of Wenzhou Medical University, and access can be provided upon request to the authors.

Ethical Approval

Ethical approval for this study was obtained from the Ethics Committee of the First Affiliated Hospital of Wenzhou Medical University.

Funding

This work was supported by the Natural Science Foundation of Zhejiang Province (LY18H160053, LY17H160053).

Disclosure

The authors of this research declare that they have no conflicts of interest for this work.

References

1. Siegel RL, Miller KD, Jemal A. Cancer statistics, 2020. *CA Cancer J Clin*. 2020;70(1):7–30. doi:10.3322/caac.21590
2. Howlader N, Altekruse SF, Li CI, et al. US incidence of breast cancer subtypes defined by joint hormone receptor and HER2 status. *J Natl Cancer Inst*. 2014;106:5. doi:10.1093/jnci/dju055
3. Waks AG, Winer EP. Breast cancer treatment: a review. *JAMA*. 2019;321(3):288–300. doi:10.1001/jama.2018.19323

4. Prat A, Saura C, Pascual T, et al. Ribociclib plus letrozole versus chemotherapy for postmenopausal women with hormone receptor-positive, HER2-negative, luminal B breast cancer (CORALLEEN): an open-label, multicentre, randomised, Phase 2 trial. *Lancet Oncol*. 2020;21(1):33–43. doi:10.1016/S1470-2045(19)30786-7
5. von Minckwitz G, Procter M, de Azambuja E, et al. Adjuvant pertuzumab and trastuzumab in early HER2-positive breast cancer. *N Engl J Med*. 2017;377(2):122–131. doi:10.1056/NEJMoa1703643
6. DeSantis CE, Ma J, Gaudet MM, et al. Breast cancer statistics, 2019. *CA Cancer J Clin*. 2019;69(6):438–451. doi:10.3322/caac.21583
7. Lim B, Hortobagyi GN. Current challenges of metastatic breast cancer. *Cancer Metastasis Rev*. 2016;35(4):495–514. doi:10.1007/s10555-016-9636-y
8. Jin-Kyeoung Kim RR, Ishizuka Y, Kato S. Identification of cDNAs encoding two novel nuclear proteins, IMUP-1 and IMUP-2, upregulated in SV40-immortalized human fibroblasts. *Gene*. 2000;257:237–344.
9. Jeon SY, Lee HJ, Park JM, et al. Increased immortalization-upregulated protein 2 (IMUP-2) by hypoxia induces apoptosis of the trophoblast and pre-eclampsia. *J Cell Biochem*. 2010;110(2):522–530. doi:10.1002/jcb.22568
10. Jeon SY, Lee HJ, Na KH, et al. Hypoxia-induced downregulation of XIAP in trophoblasts mediates apoptosis via interaction with IMUP-2: implications for placental development during pre-eclampsia. *J Cell Biochem*. 2013;114(1):89–98. doi:10.1002/jcb.24304
11. Kim JK, An HJ, Kim NK, et al. IMUP-1 and IMUP-2 genes are up-regulated in human ovarian epithelial tumors. *Anticancer Res*. 2003;23(6C):4709–4713.
12. Kim SJ, An HJ, Kim HJ, et al. Imup-1 and imup-2 overexpression in endometrial carcinoma in Korean and Japanese populations. *Anticancer Res*. 2008;28(2A):865–871.
13. Klopp AH, Jhingran A, Ramdas L, et al. Gene expression changes in cervical squamous cell carcinoma after initiation of chemoradiation and correlation with clinical outcome. *Int J Radiat Oncol Biol Phys*. 2008;71(1):226–236. doi:10.1016/j.ijrobp.2007.10.068
14. Guo L, Zhang K, Bing Z. Application of a coexpression network for the analysis of aggressive and nonaggressive breast cancer cell lines to predict the clinical outcome of patients. *Mol Med Rep*. 2017;16(6):7967–7978. doi:10.3892/mmr.2017.7608
15. Zhang T-G, Wu Y-Q, Pan X-B, Qu G-M, Zhang T-G. The identification of multifocal breast cancer-associated long non-coding RNAs. *Eur Rev Med Pharmacological Sci*. 2017;21:5648–5654. doi:10.26355/eurrev_201712_14008
16. Bauer JA, Chakravarthy AB, Rosenbluth JM, et al. Identification of markers of taxane sensitivity using proteomic and genomic analyses of breast tumors from patients receiving neoadjuvant paclitaxel and radiation. *Clin Cancer Res*. 2010;16(2):681–690. doi:10.1158/1078-0432.CCR-09-1091
17. Curtis C, Shah SP, Chin SF, et al. The genomic and transcriptomic architecture of 2000 breast tumours reveals novel subgroups. *Nature*. 2012;486(7403):346–352. doi:10.1038/nature10983
18. Xiao-Jun MSD, Elizabeth R, Mark E, Sgroi DC. Gene expression profiling of the tumor microenvironment during breast cancer progression. *Breast Cancer Res*. 2009;11(118).
19. Richardson AL, Wang ZC, De Nicolo A, et al. X chromosomal abnormalities in basal-like human breast cancer. *Cancer Cell*. 2006;9(2):121–132. doi:10.1016/j.ccr.2006.01.013
20. Weinberg D, Weinberg RA. The Hallmarks of Cancer. *Cell*. 2000;100:57–70. doi:10.1016/S0092-8674(00)81683-9
21. Nieto MA, Huang RY, Jackson RA, Thiery JP. Emt: 2016. *Cell*. 2016;166(1):21–45. doi:10.1016/j.cell.2016.06.028
22. Testa U, Castelli G, Pelosi E. Breast cancer: a molecularly heterogenous disease needing subtype-specific treatments. *Med Sci*. 2020;8:1.
23. Uchiyama S, Itoh H, Naganuma S, et al. Enhanced expression of hepatocyte growth factor activator inhibitor type 2-related small peptide at the invasive front of colon cancers. *Gut*. 2007;56(2):215–226. doi:10.1136/gut.2005.084079
24. Harbeck N, Gluz O. Neoadjuvant therapy for triple negative and HER2-positive early breast cancer. *Breast*. 2017;S99–S103.
25. Fujii T, Le Du F, Xiao L, et al. Effectiveness of an adjuvant chemotherapy regimen for early-stage breast cancer. *JAMA Oncol*. 2015;1:9. doi:10.1001/jamaoncol.2015.3062
26. Untch M, Konecny GE, Paepke S, von Minckwitz G. Current and future role of neoadjuvant therapy for breast cancer. *Breast*. 2014;23(5):526–537. doi:10.1016/j.breast.2014.06.004
27. Cortazar P, Zhang L, Untch M, et al. Pathological complete response and long-term clinical benefit in breast cancer: the CTNeoBC pooled analysis. *Lancet*. 2014;384(9938):164–172. doi:10.1016/S0140-6736(13)62422-8
28. Yuan H, Chen J, Liu Y, et al. Association of PIK3CA mutation status before and after neoadjuvant chemotherapy with response to chemotherapy in women with breast cancer. *Clin Cancer Res*. 2015;21(19):4365–4372. doi:10.1158/1078-0432.CCR-14-3354
29. Balko JM, Giltnane JM, Wang K, et al. Molecular profiling of the residual disease of triple-negative breast cancers after neoadjuvant chemotherapy identifies actionable therapeutic targets. *Cancer Discov*. 2014;4(2):232–245. doi:10.1158/2159-8290.CD-13-0286
30. Wang BD, Lee NH. Aberrant RNA splicing in cancer and drug resistance. *Cancers*. 2018;10:11. doi:10.3390/cancers10110458
31. Sarrio D, Rodriguez-Pinilla SM, Hardisson D, Cano A, Moreno-Bueno G, Palacios J. Epithelial-mesenchymal transition in breast cancer relates to the basal-like phenotype. *Cancer Res*. 2008;68(4):989–997. doi:10.1158/0008-5472.CAN-07-2017
32. OD I, MD K, Arpaci F, Atalay C, Pak I, Gündüz U. Drug resistant MCF-7 cells exhibit epithelial-mesenchymal transition gene expression pattern. *Biomed Pharmacother*. 2011;65(1):40–45. doi:10.1016/j.biopha.2010.10.004
33. Yang Q, Huang J, Wu Q, et al. Acquisition of epithelial-mesenchymal transition is associated with Skp2 expression in paclitaxel-resistant breast cancer cells. *Br J Cancer*. 2014;110(8):1958–1967. doi:10.1038/bjc.2014.136